Atmospheric Environment 90 (2014) 78–86

Contents lists available at ScienceDirect

Atmospheric Environment

journal homepage: www.elsevier.com/locate/atmosenv

# A size-segregation method for monitoring the diurnal characteristics of atmospheric black carbon size distribution at urban traffic sites

Yu-Hsiang Cheng [a,*], Chung-Wen Liao [a], Zhen-Shu Liu [a], Chuen-Jinn Tsai [b], Hsing-Cheng Hsi [c]

[a] Department of Safety, Health and Environmental Engineering, Ming Chi University of Technology, 84 Gungjuan Rd, Taishan, New Taipei 24301, Taiwan
[b] Institute of Environmental Engineering, National Chiao Tung University, 1001 University Rd, Hsinchu 30010, Taiwan
[c] Graduate Institute of Environmental Engineering, National Taiwan University, 71 Jhoushan Rd., Daan, Taipei 10673, Taiwan

## HIGHLIGHTS

- A novel method for determining the mass size distribution of BC is developed.
- 90% of BC aerosols are smaller than 0.5 μm at urban traffic sites.
- Most BC aerosols are in the size range of 0.1–0.25 μm.
- Size distribution of BC exhibits a single mode at 0.16 μm at this sampling site.

## ARTICLE INFO

*Article history:*
Received 28 November 2013
Received in revised form
8 March 2014
Accepted 11 March 2014
Available online 12 March 2014

*Keywords:*
Black carbon
Size segregation
Mass size distribution
Taipei urban area

## ABSTRACT

Understanding the characteristics of the size distribution of ambient black carbon (BC) in distinct environments is critical because the influence of BC aerosols on climate, visibility, and human health depends strongly on the distribution of BC aerosols over the particle size spectrum. In this study, a novel method for determining the mass size distribution of BC in atmospheric aerosols was developed. This size-segregation method relies on measuring BC in parallel using two aethalometers, one of which is used to measure the total BC ($BC_T$) mass concentration as a reference level and the other is used to measure the BC ($BC_i$) mass concentration for BC sizes below specific particle sizes that are selected using a size cut-off inlet. In this study, this method was applied to measure BC in atmospheric samples at an urban traffic site. The aethalometers were operated continually from December 15, 2012 to January 31, 2013, and from February 15, 2013 to March 31, 2013. The measurement results presented in this paper are for the diurnal variation patterns, average concentrations, mass fractions, and size distributions of BC aerosols. The results indicate that $BC_T$ mass concentration is approximately 2.8 μg $m^{-3}$ in the Taipei urban area. The levels of BC at this sampling site were affected markedly by traffic emission levels and local wind speed. At the sampling site, the average $BC_{2.5}/BC_T$, $BC_{1.0}/BC_T$, $BC_{0.5}/BC_T$, $BC_{0.25}/BC_T$, and $BC_{0.1}/BC_T$ were 0.96 ± 0.04, 0.92 ± 0.07, 0.89 ± 0.04, 0.73 ± 0.10, and 0.18 ± 0.08, respectively. The results indicate that approximately 90% of the BC aerosols were smaller than 0.5 μm, that most of the BC aerosols (55%) were in the size range of 0.1–0.25 μm, and that approximately 18% of the BC aerosols were ultrafine. Moreover, the daily average mass size distribution of BC exhibited a single accumulation mode at 0.16 μm at this sampling site. The mode of the BC mass size distribution at rush hour (9 AM) was only 0.14 μm, which is smaller than the daily average. Moreover, the mode of the BC mass size distribution at an early morning hour (3 AM) was 0.18 μm, and a minor coarse mode was also observed during this period. The results further revealed that the geometric diameter ($D_{pg}$) of the BC aerosols varied between 0.14 and 0.22 μm and the geometric standard deviation ($\sigma_g$) of these BC aerosols ranged between 1.4 and 2.3 during the sampling period. Because BC exhibits extremely low chemical reactivity; the size distribution of BC in the atmosphere does not change substantially except through coagulation.



* Corresponding author.
*E-mail address:* yhcheng@mail.mcut.edu.tw (Y.-H. Cheng).

http://dx.doi.org/10.1016/j.atmosenv.2014.03.023
1352-2310/

## 1. Introduction

Black carbon (BC) is a major component of aerosols produced by the incomplete combustion of carbonaceous fuels. BC plays a key role in aerosol climatic forcing because it exhibits light-absorption properties (Bond and Bergstrom, 2006; Jacobson, 2010). Ramanathan and Carmichael (2008) noted that the direct radiative forcing of BC can be high as +0.9 W $m^{-2}$ and can be higher than the radiative forcing of other greenhouse gases such as $CH_4$, CFCs, $N_2O$, and tropospheric ozone. Furthermore, BC can cause numerous respiratory diseases and adversely affect the cardiovascular system because submicron BC particles can penetrate deep into the lungs and be deposited on the pulmonary alveolus (Suglia et al., 2008; Power et al., 2011; Cornell et al., 2012). Therefore, BC emissions are both a regional and global concern. Bond et al. (2013) reported that the global emissions of BC in 2000 were as high as 7.6 Tg, with approximately 27% of the BC being derived from diesel engines, 25% from residential solid fuel, 40% from open burning, and 8% from other sources such as ship emissions. However, large uncertainties exist regarding BC emissions because of insufficient field data, particularly in Asia. Ramanathan and Carmichael (2008) reported that BC emissions from China and India accounted for roughly 30% of global emissions. Zhang et al. (2009) suggested that the total BC emissions in Asia in 2006 were approximately 3.0 Tg, and that the BC emissions from China accounted for 1.8 Tg. Despite these discrepancies in the measurements of BC emissions, lowering BC emission represents a potential mitigation strategy that could reduce the global climate forcing caused by anthropogenic activities in the short term, and slow the associated rate of climate change and diminish the effect of BC on air quality and human health.

To develop strategies to control atmospheric BC, understanding the characteristics of the ambient BC size distributions in distinct environments is critical; this is because the influence of BC aerosols on climate, visibility, and human health strongly depends on the distribution of the BC aerosols over the particle size spectrum. However, the database on ambient BC size distributions is more limited than the database on total BC mass concentrations. Impactors have been used to collect size-segregated aerosol samples for BC analysis (Hitzenberger and Tohno, 2001; Viidanoja et al., 2002a; Mallet et al., 2003; Cuccia et al., 2013), but BC particle size distributions measured using the impactor have not provided results that exhibit adequate time resolution. Recently, a single particle soot photometer (SP2; Droplet Measurement Technologies) has been used to measure BC size distributions in real time by using the laser-induced incandescence technique (Schwarz et al., 2006; Shiraiwa et al., 2008; Schwarz et al., 2008; Kondo et al., 2011). However, SP2 is not widely used for studying BC in atmospheric aerosols because of the cost and performance limitations of SP2 (Gysel et al., 2012). Lately, a differential mobility analyzer (DMA) combined with an aethalometer had been applied to determine BC mass size distributions by using the different electrical mobility and light absorption methods (Stabile et al., 2012; Ning et al., 2013). This DMA-aethalometer system can be used to determine the BC modal characteristics directly in the size range of 20–600 nm.

The most common method used to measure BC involves collecting aerosols on a filter and measuring the reduction in light transmission through the filter (Hansen et al., 1984). The aethalometer (AE; Magee Scientific), multiangle absorption photometer (MAAP; Thermo Scientific), and particle soot absorption photometer (PSAP; Radiance Research) are among the currently available devices used for measuring BC by using filter-based optical techniques. These devices have been used extensively to monitor environmental BC mass concentrations because they can be operated easily and they provide favorable time resolution (Watson et al., 2005; Park et al., 2006; Chow et al., 2009). In this study, a method for determining the mass size distribution of BC in atmospheric aerosols was developed. This size-segregation method relies on measuring BC in parallel using two aethalometers; one of the two devices is used to measure the total BC mass concentration as a reference level, whereas the other is used to measure the BC mass concentration for BC sizes below specific particle sizes selected using a size cut-off inlet. The mass fractions of BC at various cut-off sizes in total BC can be determined using this size-segregated method, and the BC size distribution can be subsequently evaluated using these mass fraction data under various size ranges. One valuable feature of this method is that it offers time resolution for assessing BC mass size distribution. In this study, this method was applied to measure BC in atmospheric samples at an urban traffic site. The measurement results reveal the diurnal variation patterns, average concentrations, mass fractions and size distributions of BC aerosols.

## 2. Methods

### 2.1. Sampling equipment and data collection

In this study, two aethalometers (AE31; Magee Scientific) were used concurrently to measure BC mass concentrations at a traffic site. The sampling site (25° 04′ 20″ N; 121° 53′ 75″ E) used in this study is located on the campus of National Taipei University of Technology at Daan, Taipei, Taiwan, which is near the intersection of Jianguo Expressway and Zhongxiao E. Rd. (Fig. 1). Jianguo Expressway and Zhongxiao E. Rd. are north-south and east-west arterial roads, respectively, in Taipei City. Jianguo Expressway is linked to Taipei's road network and Zhongxiao E. Rd. connects two major commercial areas of Taipei City, the east and west commercial districts. Moreover, the east-west Civic Expressway is located 300 m north of the sampling site. Consequently, traffic is the primary local source of atmospheric particulate matter at this sampling site.

BC was measured in parallel using two aethalometers in this study; one aethalometer (Aethalometer A) was used to measure the total BC ($BC_T$) mass concentration as a reference level, whereas the other (Aethalometer B) was used to measure the BC mass concentrations for BC sizes below selected particle sizes (Fig. 2). The five cut-off sizes chosen in this study were 2.5, 1.0, 0.5, 0.25, and 0.1 μm, and the measured BC mass concentrations at these sizes were represented as $BC_{2.5}$, $BC_{1.0}$, $BC_{0.5}$, $BC_{0.25}$, and $BC_{0.1}$, respectively. The cut-off inlets of the various sizes used in this study for Aethalometer B are listed in Table 1. The $PM_{2.5}$ and $PM_{1.0}$ cyclones (BGI Inc.) had cut-off diameters of 2.5 and 1.0 μm, respectively, at a sampling flow rate of 5 L $min^{-1}$. These two cyclones were used to

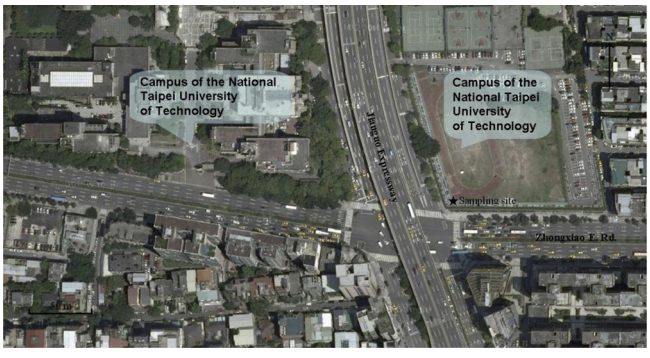


**Fig. 1.** Location of the sampling site on the campus of the National Taipei University of Technology.

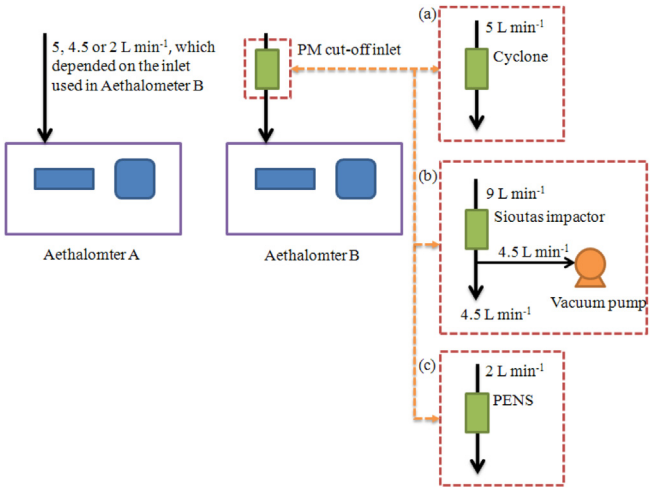


**Fig. 2.** Schematic diagram of the measurement system.

determine the $BC_{2.5}$ and $BC_{1.0}$, respectively. The Sioutas cascade impactor (SKC Inc.) consisted of four impaction stages and an after-filter. The cut-off diameters used for these four impaction stages were 2.5, 1.0, 0.5 and 0.25 μm under a sampling flow rate of 9 L $min^{-1}$. In this study, the downstream filter and the filter-support screen were not installed inside the Sioutas cascade impactor and, thus, particles below the last stage were collected on the filter of Aethalometer B. The flow rate through the Sioutas cascade impactor was controlled at 9.0 L $min^{-1}$. Downstream of the Sioutas cascade impactor, a Y-type flow splitter was used to separate the flow streams equally. One of two divided flow streams was introduced into Aethalometer B and the other was drawn using an external pump, the flow rate of which was tightly controlled using a critical orifice. In this study, the Sioutas cascade impactor that without the fourth stage was used to determine the $BC_{0.5}$. When the all stages were installed in Sioutas cascade impactor, it was used to determine the $BC_{0.25}$. Additionally, the personal nanoparticle sampler (PENS) used in this study was developed by Tsai et al. (2012); the PENS consists of a respirable cyclone and a micro-orifice impactor featuring cut-off diameters of 4 and 0.1 μm, respectively, at a sampling flow rate of 2 L $min^{-1}$. In this study, PENS was used to determine the $BC_{0.1}$. To prevent particles from bouncing off the impaction surface, the impaction substrates were coated with silicon oil; moreover, the impaction substrates in the impactor used in this study were replaced with new substrates every 8 h.

During the sampling periods, the two aethalometers were set at the same sampling flow rate (2, 4.5 or 5.0 L $min^{-1}$), which depended on the inlet used in Aethalometer B. The cut-off inlets of each size were used individually as the sampling inlet in Aethalometer B, and the BC mass concentrations at each specific size cut-off inlet were measured continuously for approximately 2 weeks. The two aethalometers were positioned adjacent to each other in a sampling cabin and the inlets of both the aethalometers were approximately 2 m above ground level outside the sampling cabin. The aethalometers were operated continually from December 15, 2012 to January 31, 2013, and from February 15, 2013 to March 31, 2013. The logging interval used for all of the measurements was set at 5 min. Local meteorological data such as wind speed and direction, temperature, and relative humidity were recorded using a Vantage Pro 2™ Weather Station (Davis Instruments). Wind speed and direction were measured at a height of 3 m above the ground.

**Table 1**
The cut-off inlets of the various sizes used in this study.

| Sampling inlet | Cut-off diameter | Sampling flow rate |
|---|---|---|
| BGI $PM_{2.5}$ cyclone | 2.5 μm | 5 L $min^{-1}$ |
| BGI $PM_{1.0}$ cyclone | 1.0 μm | 5 L $min^{-1}$ |
| SKC Sioutas cascade impactor[a] | 0.5 μm | 9 L $min^{-1}$ |
| SKC Sioutas cascade impactor | 0.25 μm | 9 L $min^{-1}$ |
| Personal nanoparticle sampler (PENS) | 0.1 μm | 2 L $min^{-1}$ |

[a] The fourth stage in the impactor was not installed.

### 2.2. Data analysis

BC mass concentrations measured using aethalometers can be underestimated when particles load onto the filter (Weingartner et al., 2003). In this study, the filter tape in the aethalometer was advanced automatically to expose a new spot on the filter every 2 h to maintain a low filter loading during the sampling periods. However, the loading effects can be accounted for using an empirical correction scheme. Virkkula et al. (2007) developed a simple procedure to correct for the loading effects included in aethalometer data; this correction algorithm was adopted in this study, and the correction equation can be expressed as

$$BC_{corrected} = [1 + k \cdot ATN] \cdot BC_{measured} \quad (1)$$

where $BC_{corrected}$ and $BC_{measured}$ are the BC mass concentration corrected for the loading effect and the measured BC mass concentration, respectively, in μg $m^{-3}$; ATN is the attenuation value; and $k$ is the correction factor in the algorithm. In this study, the BC mass concentrations were evaluated using 880 nm wavelength light. All of the sampling data obtained from the two aethalometers were corrected using this algorithm. Based on the analytical results, the averaged $k$ factor was determined to be 0.0033, and it was similar to previous studies (Park et al., 2010; Cheng and Lin, 2013). Park et al. (2010) suggested that correcting factor for urban site was 0.0028.

Before beginning field sampling, the performances of the two aethalometers used in this study were compared at the sampling site using the same sampling flow rate; the performance levels were compared for 2–3 days at flow rates of 2 and 5 L $min^{-1}$. The hourly measured results obtained for the two aethalometers are shown in Fig. 3. The hourly average BC mass concentrations were calculated using 5-min raw data. The statistical results indicated that the intercepts were −0.019 (95% CI: −0.044 to 0.005) and −0.026 (95% CI: −0.051 to −0.001) for the flow rates of 2 and 5 L $min^{-1}$, respectively, and the intercepts were not significantly different from zero ($p = 0.121$ for 2 L $min^{-1}$ and $p = 0.042$ for 5 L $min^{-1}$). The slopes determined for the flow rates of 2 and 5 L $min^{-1}$ were 0.987 (95% CI: 0.979–0.996) and 0.989 (95% CI: 0.983–0.995), respectively, and the slopes were significantly different from 1.0 ($p < 0.001$ for both). These comparison results demonstrated that the disparities in the BC mass concentrations measured using the two aethalometers could be negligible because of the difference in the measurement data before and after corrected was only <1%.

The hourly size-segregated mass fractions of BC corresponding to $BC_{2.5}/BC_T$, $BC_{1.0}/BC_T$, $BC_{0.5}/BC_T$, $BC_{0.25}/BC_T$, and $BC_{0.1}/BC_T$ were determined from the all measurement results using the two aethalometers. Next, the BC size distribution was calculated accurately by integrating the mass differential, term-by-term, over the measured particle size range. The geometric diameter ($D_{pg}$) and the geometric standard deviation ($\sigma_g$) of the measured BC size distribution data were evaluated by applying a lognormal function using DistFit software (Chimera Tech).

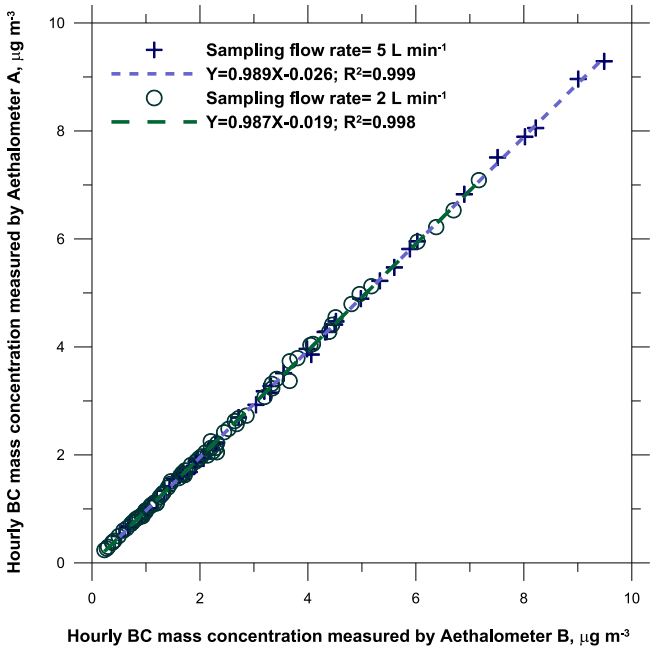


**Fig. 3.** The hourly BC mass concentration measurements of the Aethalometer B vs. Aethalometer A.

## 3. Results and discussion

### 3.1. BC mass concentrations at the sampling site

During the sampling period, the mean wind speed was 1.2 m $s^{-1}$ and the prevailing wind directions at the sampling site were north-northeast (NNE, approximately 38%) and northeast (NE, approximately 35%). Wind speed was low during the early morning hours and was typically high in the afternoon. The mean temperature and relatively humidity were 20 °C and 68%, respectively.

BC concentrations in urban areas had been determined to be 1.0–7.5 μg $m^{-3}$ in previous studies (Fruin et al., 2008; Boogaard et al., 2011; Invernizzi et al., 2011; Reche et al., 2011; Cheng et al., 2013; Rattigan et al., 2013). However, BC concentrations can be as high as a few tens of μg $m^{-3}$ in heavily polluted environments under unfavorable meteorological conditions (Dutkiewicz et al., 2009; Doumbia et al., 2012; Sharma et al., 2012; Begum et al., 2012). Table 2 summarizes the levels of hourly $BC_T$ at the sampling site. During the sampling period, the mean $BC_T$ mass concentration was 2.8 μg $m^{-3}$. The $BC_T$ mass concentration peaked during the morning hours (8:00–11:00 AM) and dipped to its lowest level during in predawn hours (1:00–5:00 AM). The $BC_T$ concentrations during the morning hours and predawn hours were approximately 3.9 μg $m^{-3}$ and 1.8 μg $m^{-3}$, respectively, and the concentrations during the morning hours was approximately 2.2 times of that during the predawn hours. The $BC_T$ concentration peaked in the morning because of local traffic emissions, whereas a diminished production of BC aerosols and their removal through deposition reduced the BC aerosol load during the predawn hours.

**Table 2**
Hourly mass concentrations of $BC_T$ at the sampling site.

| | Mean[a] (S.D.[b]) | Min–Max[c] | Median | $Q_1$–$Q_3$[d] |
|---|---|---|---|---|
| $BC_T$, μg $m^{-3}$ | 2.76 (1.84) | 0.13–12.09 | 2.27 | 1.45–3.63 |

[a] Observation number $N = 1829$.
[b] Standard deviation.
[c] Minimal value–maximal value.
[d] First quartile value–third quartile value.

These measurement results indicated that local traffic was the principal source of fresh BC, which contributed approximately 54% of the BC at this sampling site. This agrees with the results obtained by Cheng et al. (2013), who demonstrated that the BC concentration was approximately 3.5 μg $m^{-3}$ in the Taipei urban area and that the variations in BC concentration were markedly influenced by traffic emissions.

The polar plots of $BC_T$ mass concentrations during the daylight and night-time periods at the sampling site are presented in Fig. 4. The simulation results suggest that the emission sources potentially elevated $BC_T$ mass concentrations at the sampling site; this is because a major proportion of the BC distributions was measured when the wind speed was <1 m $s^{-1}$ and the wind was blowing from the southwest (SW), particularly during daylight hours. This result indicates that the long-range transport of BC did not contribute as much as the local sources did to the total amount of BC and that the primary source of BC at this sampling site was traffic. In addition to local traffic, wind speed affected the BC mass concentration in the atmosphere substantially. Fig. 5 presents the relationship between wind speed and $BC_T$ mass concentration at the sampling site. The measured results demonstrate that $BC_T$ decreased when the wind speed increased. $BC_T$ mass concentrations >4.5 μg $m^{-3}$ were observed under calm condition; however, when the wind speed was >2 m $s^{-1}$, the $BC_T$ concentrations fell to <2.0 μg $m^{-3}$. Thus, the atmospheric dilution of BC aerosols caused by wind was considerable, particularly in the afternoon. These results indicating the effect of wind speed on BC agree with the results obtained by Pakkanen et al. (2000), Viidanoja et al. (2002b), Rodríguez et al. (2008), Wang et al. (2011), and Begum et al. (2012), who demonstrated that BC levels decreased exponentially with an increase in wind speed.

The diurnal variations in $BC_T$ mass concentrations on workdays, Saturdays, and Sundays measured during the sampling period are presented in Fig. 6. The average $BC_T$ mass concentrations were 2.9 μg $m^{-3}$ on workdays, 2.4 μg $m^{-3}$ on Saturdays, and approximately 2.2 μg $m^{-3}$ on Sundays. Except during the predawn hours, the $BC_T$ mass concentrations on workdays were higher than those on Saturdays and Sundays. The diurnal variations in $BC_T$ mass concentrations did not differ on both Saturdays and Sundays except during the morning hours. On workdays, the $BC_T$ mass concentrations demonstrated a clear diurnal variation, with the highest hourly average values occurring during the morning rush hours. A major peak of $BC_T$ was also observed during the morning hours on Saturdays, but this peak was slightly delayed compared with that on workday mornings. After the morning rush hours, the $BC_T$ mass concentrations decreased during the afternoon hours, likely because of the boundary layer dynamics and a lower traffic volume. The measurement results revealed that the amount of BC emitted as a result of anthropogenic activities were considerably lower on Sundays compared with those emitted on workdays and Saturdays, which suggests that the BC sources at this sampling site were transportation-related activities. Similar results were obtained by Järvi et al. (2008), Wang et al. (2011) and Pereira et al. (2012). Järvi et al. (2008) reported that the effect of traffic was evident on weekdays when maximal BC concentrations were measured during the morning and afternoon rush hours in Helsinki, Finland. The afternoon peaks were typically lower than the morning peaks because of stronger turbulent mixing and an increased mixing of layer heights occurred in the afternoon. The diurnal pattern produced on weekdays differed markedly from that produced on weekdays; minimal BC values were measured early in the morning and maximal values were produced at night and in the afternoon. Wang et al. (2011) reported that the diurnal variations of BC concentrations in Rochester, USA exhibited a primary early peak related to the morning commute and a secondary night-time peak

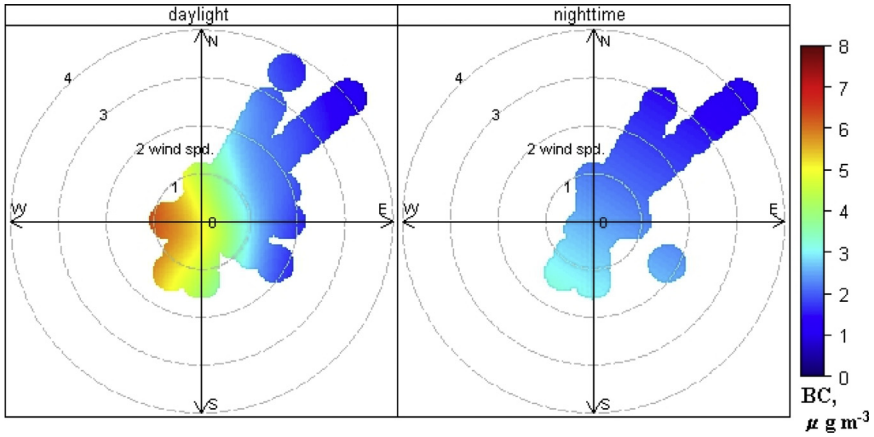


**Fig. 4.** The polar plots of $BC_T$ mass concentrations during the daylight and night-time periods at this sampling site.

was observed on weekdays. Moreover, the morning peak of BC concentrations on weekends was substantially lower than that which occurred on weekday mornings, whereas the peak at night on weekends was slightly higher than that occurring on weekday nights. Pereira et al. (2012) observed two maxima of BC concentrations in the early morning and evening hours, both of which were related to the local traffic rush hours on weekdays in the Southwestern Iberia Peninsula. The distinction between these daily variations was observed on weekdays and weekends. On weekdays, the daily variations in BC concentration were related to regular human activities in the city. On weekends, the anthropogenic activities were considerably diminished, particularly with respect to traffic, which resulted in reduced BC concentrations.

### 3.2. Hourly size-segregated mass fractions of BC at the sampling site

Fig. 7 presents the diurnal variations in the mass fractions of $BC_i$ in $BC_T$ on workdays, Saturdays, and Sundays that were calculated for the various selected sizes throughout the sampling period. At the sampling site, the average $BC_{2.5}/BC_T$, $BC_{1.0}/BC_T$, $BC_{0.5}/BC_T$, $BC_{0.25}/BC_T$, and $BC_{0.1}/BC_T$ were 0.96 ± 0.04, 0.92 ± 0.07, 0.89 ± 0.04, 0.73 ± 0.10, and 0.18 ± 0.08, respectively. The measurement results revealed that approximately 90% of the BC aerosols were smaller than 0.5 μm at this sampling site, and that most of the BC aerosols (55%) were in the size range of 0.1–0.25 μm. Approximately 18% of the BC aerosols were ultrafine. These results indicate that most of the atmospheric BC resides in the fine particle size range. A similar result was presented by Viidanoja et al. (2002b), who demonstrated that typically >90% of BC resided in the $PM_{2.5}$ size fraction at a traffic site in Helsinki, Finland. In this study, the BC in the $PM_{2.5}$ size fraction was >95%. Moreover, the percentages of ultrafine BC aerosols that were measured on workdays and Saturdays were higher than those measured on Sundays. A peak of ultrafine BC aerosols was measured during the morning hours; by contrast, the percentage of ultrafine BC aerosols was low during the predawn hours. Approximately 6–7% of BC aerosols were in the coarse size range (>2.5 μm) during the predawn and afternoon hours on Sundays, which was higher than that of the BC aerosols observed on workdays and Saturdays.

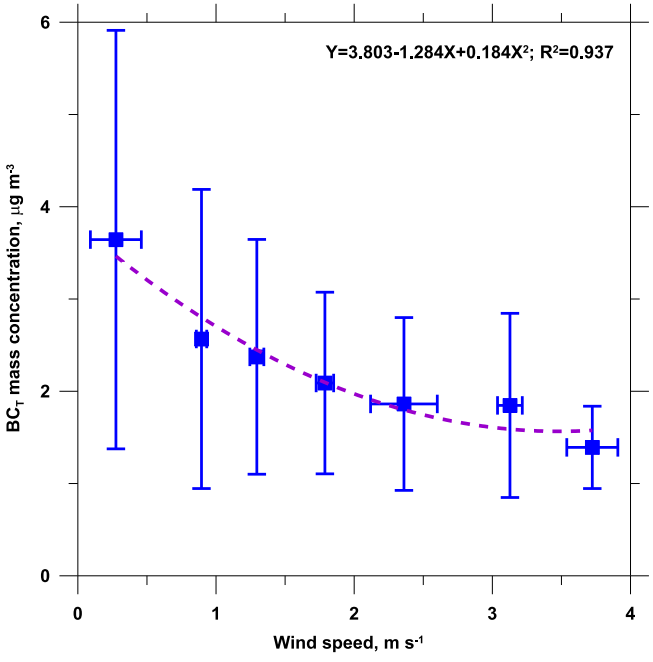


**Fig. 5.** The relationship between wind speed and $BC_T$ mass concentration at the sampling site.

Impactors have been widely used to collect size-segregated aerosol samples for subsequent BC analysis (Hitzenberger and Tohno, 2001; Viidanoja et al., 2002a; Mallet et al., 2003; Cuccia et al., 2013). Hitzenberger and Tohno (2001) noted that the BC size distribution mode was approximately 0.15–0.4 μm at two urban sites in Uji, Japan and Vienna, Austria. Viidanoja et al. (2002a) demonstrated that the distribution of BC typically displayed a single mode with a maximum between 0.1 and 0.5 μm, although a minor supermicron BC peak was also identified in a few measurements obtained at an urban site in Vallila, Helsinki. Mallet et al. (2003) reported that the mass size distribution of BC exhibited two modes, in which the major accumulation mode and minor coarse mode were approximately 0.2–0.3 and 2–3 μm, respectively, in a periurban area in Marseille, France. Cuccia et al. (2013) also demonstrated that the mass size of BC displayed a two-mode distribution, with a main mode at approximately 0.15 μm and a small mode at approximately 0.4 μm, in an urban background site in Genoa, Italy. The disparities in the results of these studies could have arisen from the distinct size resolutions of the impactors used and the environmental conditions during the sampling process. Fig. 8 presents the average BC mass size distribution measured throughout the sampling period in this study; the results indicate that the daily average mass size distribution of BC displayed one accumulation mode at 0.16 μm at the sampling site. The mode of the BC mass size distribution at a rush hour (9 AM) was only

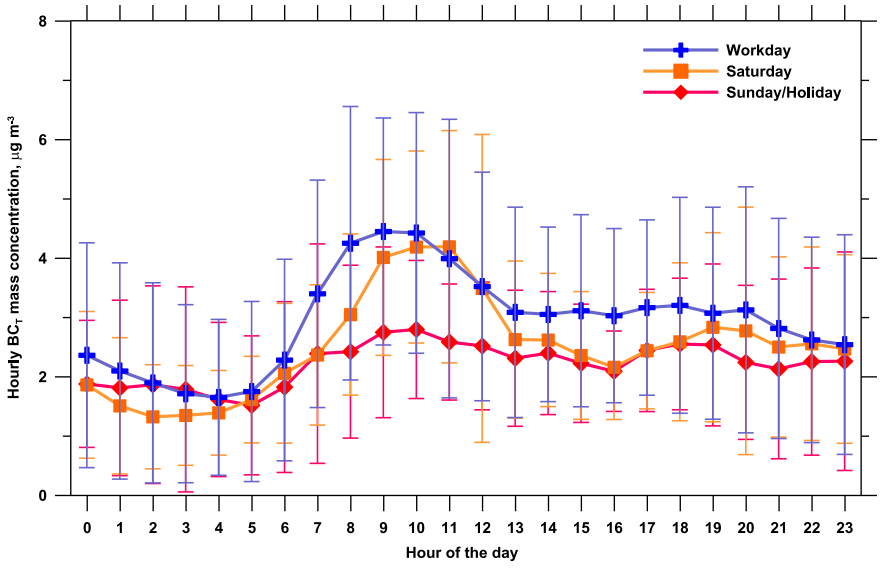


**Fig. 6.** Diurnal variations in $BC_T$ mass concentrations on workdays, Saturdays, and Sundays throughout the sampling period.

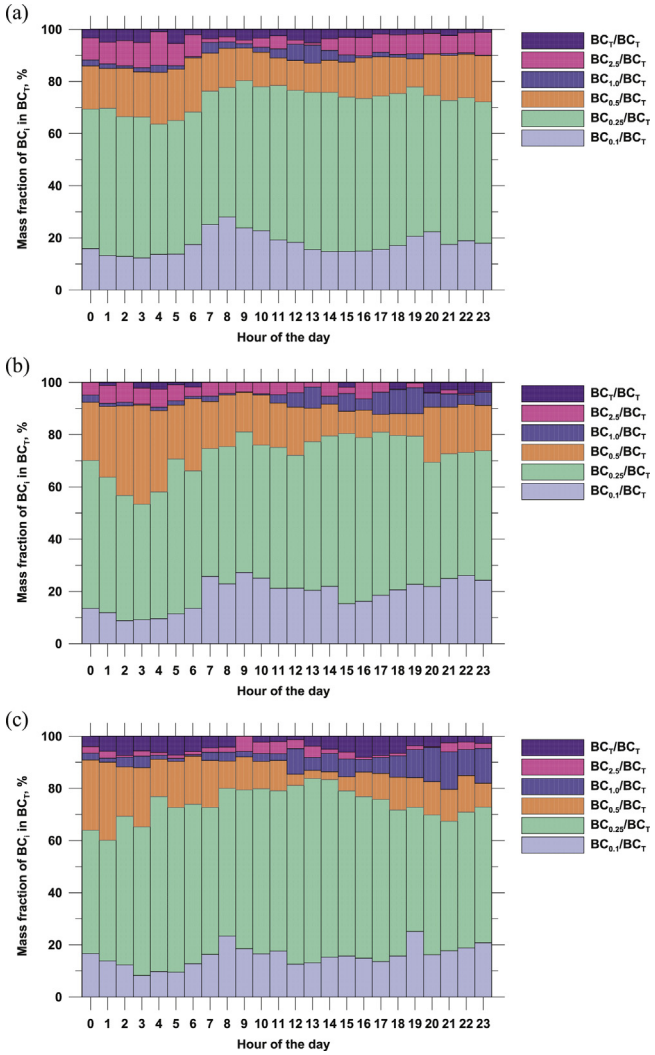


**Fig. 7.** Diurnal variations in the mass fractions of $BC_i$ in $BC_T$ for various selected sizes on (a) workdays, (b) Saturdays, and (c) Sundays throughout the sampling period.

0.14 μm, which was smaller than the daily average. Moreover, the BC mass size distribution mode at an early morning hour (3 AM) was 0.18 μm, and a minor coarse mode was also observed during this period. However, this minor coarse mode was disregarded in the bimodal lognormal function fitting performed using DistFit software. Recently, Schwarz et al. (2008) measured BC mass size distributions in Central Europe by using an SP2, and the results displayed a mass mode of approximately 0.2 μm. Kondo et al. (2011) also used an SP2 to measure the mass size distribution of BC in real time and reported that the mode of fresh BC aerosols ranged from 0.12 to 0.16 μm in the urban areas of Tokyo and Nagoya, Japan and Seoul, Korea. Lately, Ning et al. (2013) measured BC mass size distributions in the urban ambient environment and at a busy

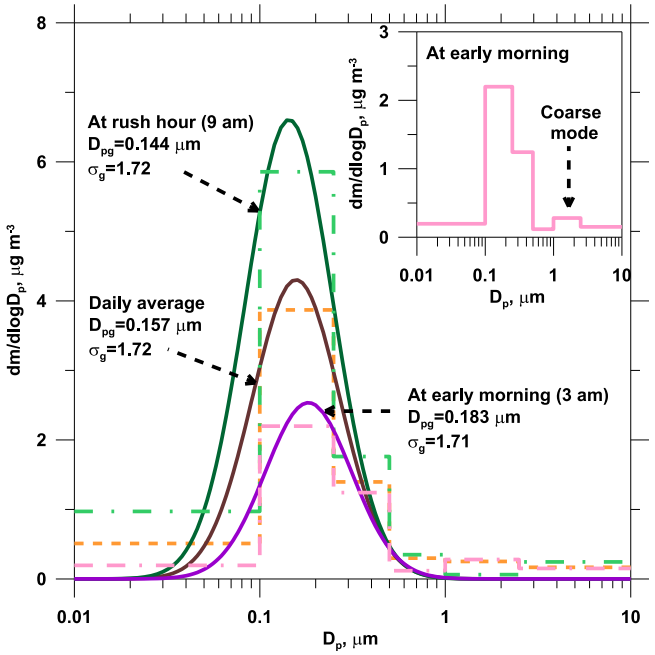


**Fig. 8.** The average BC mass size distribution measured throughout the sampling period.

roadside of Hong Kong by using a DMA-aethalometer system, and the results also displayed a mass mode around 0.2 μm for BC aerosols at these two different environments. Moreover, there could be observed a minor peak of BC mass on size <0.05 μm in some cases while using a DMA-aethalometer system to measure BC mass size distributions. The mode of the BC mass size distribution measured in this study was similar to those determined by Mallet et al. (2003), Schwarz et al. (2008) and Kondo et al. (2011), which indicates that the size-segregation method developed in this study can be used to accurately evaluate the mass size distribution of BC in the atmosphere.

Fig. 9 shows the diurnal variations in BC mass size distributions on workdays, Saturdays, and Sundays throughout the sampling period. The results demonstrate that the $D_{pg}$ of BC aerosols varied between 0.14 and 0.22 μm and that the $\sigma_g$ of BC aerosols ranged between 1.4 and 2.3. The $D_{pg}$ of BC aerosols during the daylight hours, particularly the morning hours, was markedly smaller than that of the BC aerosols during night-time hours. The $D_{pg}$ of BC aerosols was smallest during the morning hours on workdays, which indicates that most particles during these periods were fresh and produced by traffic emissions. The $D_{pg}$ values of BC aerosols measured during the morning hours were 0.14, 0.15, and 0.15 μm on workdays, Saturdays, and Sundays, respectively. The $D_{pg}$ likely increased because of the coagulation of particles during predawn hours, especially on Saturdays: the $D_{pg}$ values of BC aerosols during predawn hours were 0.17, 0.21, and 0.18 μm on workdays, Saturdays, and Sundays, respectively. Because BC exhibits extremely low chemical reactivity, the size distribution of BC in the atmosphere does not change considerably except through coagulation. Consequently, the size distributions of the BC component in ambient aerosol are affected by only the size of BC at the time of emission and by subsequent coagulation. The mass size distribution of BC emitted by engines was typically found in the Aitken mode (i.e., <0.1 μm) (Kittelson, 1998), but most of this BC was observed in the

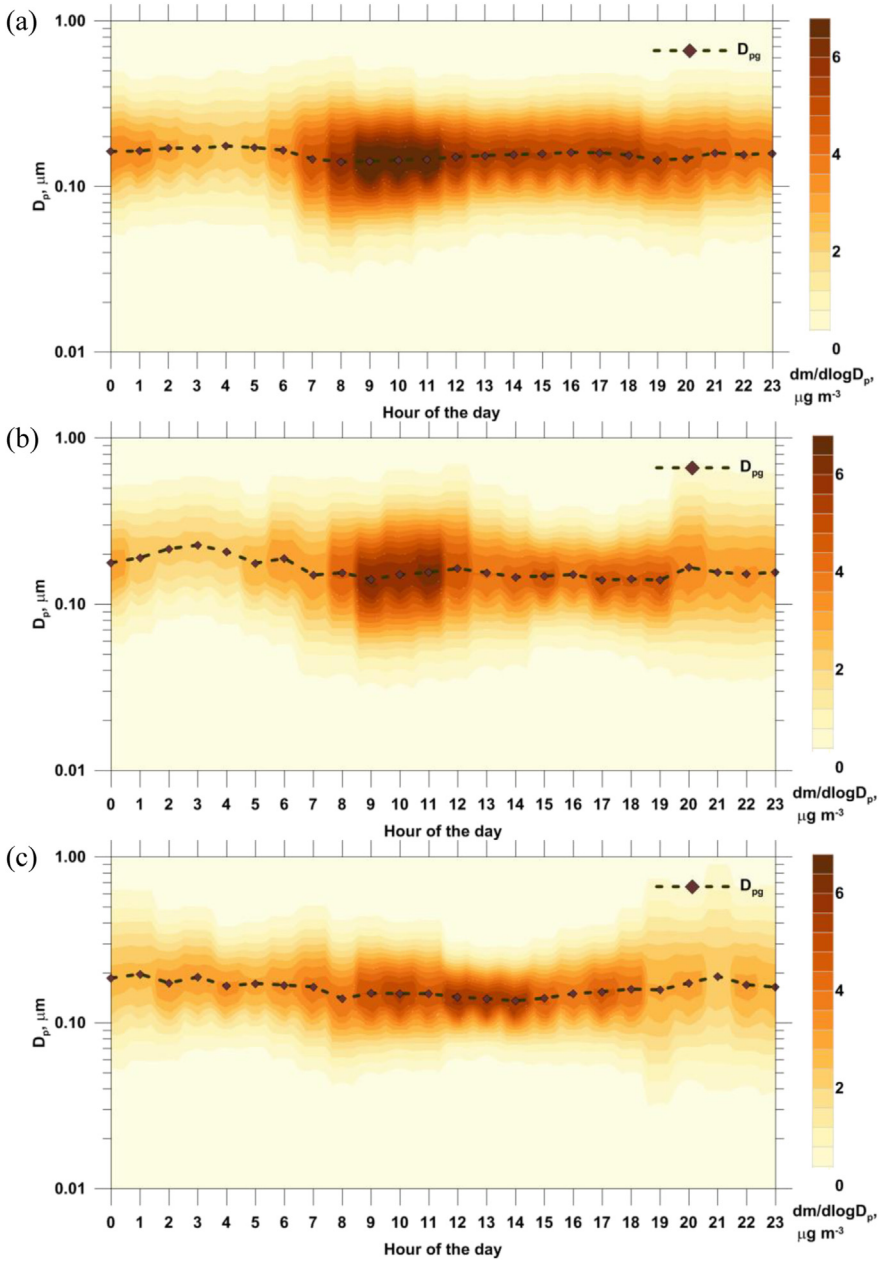


**Fig. 9.** Diurnal variations in BC mass size distributions on (a) workdays, (b) Saturdays, and (c) Sundays throughout the sampling period.

accumulation mode between 0.1 and 0.5 μm as a result of coagulation in the atmosphere. Moreover, a minor coarse mode of BC aerosols was observed in aged aerosols during the predawn hours, which suggests that the BC size increases through coagulation when the BC lingers in the atmosphere for a few hours after emissions.

## 4. Conclusions

The measurement results presented in this paper demonstrate that $BC_T$ mass concentration is approximately 2.8 μg $m^{-3}$ at a traffic site in the Taipei urban area. The levels of BC at this sampling site are strongly affected by traffic emission levels and local wind speed. The results indicate that approximately 90% of the BC aerosols are smaller than 0.5 μm at this sampling site, that most BC aerosols (55%) are in the size range of 0.1–0.25 μm, and that approximately 18% of the BC aerosols are ultrafine. The results further reveal that the $D_{pg}$ of BC aerosols varied between 0.14 and 0.22 μm and the $\sigma_g$ of BC aerosols ranged between 1.4 and 2.3 during the sampling period. The results of this study demonstrate that the size-segregation method relying on measuring BC in parallel using two aethalometers can be employed to accurately evaluate the mass size distribution of BC in the atmosphere. These temporally resolved results can be used to refine the findings used for climate modeling to determine the effect of atmospheric BC aerosols on global climate. However, the size resolution of the BC mass size distribution can be improved in future by using a high-size-resolution cascade impactor as the sampling inlet.

## Acknowledgments

The authors would like to thank the National Science Council Taiwan, for financially supporting this research under Contract No. NSC101-2221-E-131-026.

## References

Begum, B.A., Hossain, A., Nahar, N., Markwitz, A., Hopke, P.K., 2012. Organic and black carbon in $PM_{2.5}$ at an urban site at Dhaka, Bangladesh. Aerosol and Air Quality Research 12, 1062–1072.

Bond, T.C., Bergstrom, R.W., 2006. Light absorption by carbonaceous particles: an investigative review. Aerosol Science and Technology 40, 27–67.

Bond, T.C., Doherty, S.J., Fahey, D.W., Forster, P.M., Berntsen, T., DeAngelo, B.J., Flanner, M.G., Ghan, S., Karcher, B., Koch, D., Kinne, S., Kondo, Y., Quinn, P.K., Sarofim, M.C., Schultz, M.G., Schulz, M., Venkataraman, C., Zhang, H., Zhang, S., Bellouin, N., Guttikunda, S.K., Hopke, P.K., Jacobson, M.Z., Kaiser, J.W., Klimont, Z., Lohmann, U., Schwarz, J.P., Shindell, D., Storelvmo, T., Warren, S.G., Zender, C.S., 2013. Bounding the role of black carbon in the climate system: a scientific assessment. Journal of Geophysical Research – Atmospheres 118, 5380–5552.

Boogaard, H., Kos, G.P.A., Weijers, E.P., Janssen, N.A.H., Fischer, P.H., Zee, S.C., Hartog, J.J., Hoek, G., 2011. Contrast in air pollution components between major streets and background locations: particulate matter mass, black carbon, elemental composition, nitrogen oxide and ultrafine particle number. Atmospheric Environment 45, 650–658.

Cheng, Y.H., Lin, M.H., 2013. Real-time performance of the microAeth® AE51 and the effects of aerosol loading on its measurement results at a traffic site. Aerosol and Air Quality Research 13, 1853–1863.

Cheng, Y.H., Shiu, B.T., Lin, M.H., Yan, J.W., 2013. Levels of black carbon and their relationship with particle number levels – observation at an urban roadside in Taipei City. Environmental Science and Pollution Research 20, 1537–1545.

Chow, J.C., Watson, J.G., Doraiswamy, P., Chen, L.W.A., Sodeman, D.A., Lowenthal, D.H., Park, K., Arnott, W.P., Motallebi, N., 2009. Aerosol light absorption, black carbon, and elemental carbon at the Fresno Supersite, California. Atmospheric Research 93, 874–887.

Cornell, A.G., Chillrud, S.N., Mellins, R.B., Acosta, L.M., Miller, R.L., Quinn, J.W., Yan, B., Divjan, A., Olmedo, d.O.E., Lopez-Pintado, S., Kinney, P.L., Perera, F.P., Jacobson, J.S., Goldstein, I.F., Rundle, A.G., Perzanowski, M.S., 2012. Domestic airborne black carbon and exhaled nitric oxide in children in NYC. Journal of Exposure Science and Environmental Epidemiology 22, 258–266.

Cuccia, E., Massabò, D., Ariola, V., Bove, M.C., Fermo, P., Piazzalunga, A., Prati, P., 2013. Size-resolved comprehensive characterization of airborne particulate matter. Atmospheric Environment 67, 14–26.

Doumbia, E.H.T., Liousse, C., Galy-Lacaux, C., Ndiaye, S.A., Diop, B., Ouafo, M., Assamoi, E.M., Gardrat, E., Castera, P., Rosset, R., Akpo, A., Sigha, L., 2012. Real time black carbon measurements in West and Central Africa urban sites. Atmospheric Environment 54, 529–537.

Dutkiewicz, V.A., Alvi, S., Ghauri, B.M., Choudhary, M.I., Husain, L., 2009. Black carbon aerosols in urban air in South Asia. Atmospheric Environment 43, 1737–1744.

Fruin, S., Westerdahl, D., Sax, T., Sioutas, C., Fine, P.M., 2008. Measurements and predictors of on-road ultrafine particles concentrations and associated pollutants in Los Angeles. Atmospheric Environment 42, 207–219.

Gysel, M., Laborde, M., Mensah, A.A., Corbin, J.C., Keller, A., Kim, J., Petzold, A., Sierau, B., 2012. Technical Note: the single particle soot photometer fails to reliably detect PALAS soot nanoparticles. Atmospheric Measurement Techniques 5, 3017–3099.

Hansen, A.D.A., Rosen, H., Novakov, T., 1984. The aethalometer – an instrument for the real-time measurement of optical absorption by aerosol particles. Science of the Total Environment 36, 191–196.

Hitzenberger, R., Tohno, S., 2001. Comparison of black carbon (BC) aerosols in two urban areas – concentrations and size distributions. Atmospheric Environment 35, 2153–2167.

Invernizzi, G., Ruprecht, A., Mazza, R., Marco, C.D., Močnik, G., Sioutas, C., Westerdahl, D., 2011. Measurement of black carbon concentration as an indicator of air quality benefits of traffic restriction policies within the ecopass zone in Milan, Italy. Atmospheric Environment 45, 3522–3527.

Jacobson, M.Z., 2010. Short-term effects of controlling fossil-fuel soot, biofuel soot and gases, and methane on climate, Arctic ice, and air pollution health. Journal of Geophysical Research 115, D114209. http://dx.doi.org/10.1029/2009JD013795.

Järvi, L., Junninen, H., Karppinen, A., Hillamo, R., Virkkula, A., Mäkelä, T., Pakkanen, T., Kulmala, M., 2008. Temporal variations in black carbon concentrations with different time scales in Helsinki during 1996–2005. Atmospheric Chemistry and Physics 8, 1017–1027.

Kittelson, D.B., 1998. Engines and nanoparticles: a review. Journal of Aerosol Science 29, 575–588.

Kondo, Y., Sahu, L., Moteki, N., Khan, F., Takegawa, N., Liu, X., Koike, M., Miyakawa, T., 2011. Consistency and traceability of black carbon measurements made by laser-induced incandescence, thermal-optical transmittance, and filter-based photo-absorption techniques. Aerosol Science and Technology 45, 295–312.

Mallet, M., Roger, J.C., Despiau, S., Dubovik, O., Putaud, J.P., 2003. Microphysical and optical properties of aerosol particles in urban zone during ESCOMPTE. Atmospheric Research 69, 73–97.

Ning, Z., Chan, K.L., Wong, K.C., Westerdahl, D., Močnik, G., Zhou, J.H., Cheung, C.S., 2013. Black carbon mass size distributions of diesel exhaust and urban aerosols measured using differential mobility analyzer in tandem with Aethalometer. Atmospheric Environment 80, 31–40.

Pakkanen, T.A., Kerminen, V.M., Ojanen, C.H., Hillamo, R.E., Aarnio, P., Koskentalo, T., 2000. Atmospheric black carbon in Helsinki. Atmospheric Environment 34, 1497–1506.

Park, K., Chow, J.C., Watson, J.G., Trimble, D.L., Doraiswamy, P., Arnott, W.P., Stroud, K.R., Bowers, K., Bode, R., Petzold, A., Hansen, A.D.A., 2006. Comparison of continuous and filter-based carbon measurements at the Fresno Supersite. Journal of the Air & Waste Management Association 56, 474–491.

Park, S.S., Hansen, A.D.A., Cho, S.Y., 2010. Measurement of real time black carbon for investigating spot loading effects of Aethalometer data. Atmospheric Environment 44, 1449–1455.

Pereira, S.N., Wagner, F., Silva, A.M., 2012. Long term black carbon measurements in the southwestern Iberia Peninsula. Atmospheric Environment 57, 63–71.

Power, M.C., Weisskopf, M.G., Alexeeff, S.E., Coull, B.A., Spiro III, A., Schwartz, J., 2011. Traffic-related air pollution and cognitive function in a cohort of older men. Environmental Health Perspectives 119, 682–687.

Ramanathan, V., Carmichael, G., 2008. Global and regional climate changes due to black carbon. Nature Geoscience 1, 221–227.

Rattigan, O.V., Civerolo, K., Doraiswamy, P., Felton, H.D., Hopke, P.K., 2013. Long term black carbon measurements at two urban locations in New York. Aerosol and Air Quality Research 13, 1181–1196.

Reche, C., Querol, X., Alastuey, A., Viana, M., Pey, J., Moreno, T., Rodríguez, S., González, Y., Fernández-Camacho, R., Sánchez de la Campa, A.M., De la Rosa, J., Dall'Osto, M., Prévôt, A.S.H., Hueglin, C., Harrison, R.M., Quincey, P., 2011. New considerations for PM, black carbon and particle number concentration for air quality monitoring across different European cities. Atmospheric Chemistry and Physics 11, 6207–6227.

Rodríguez, S., Cuevas, E., González, Y., Ramos, R., Romero, P.M., Pérez, N., Querol, X., Alastuey, A., 2008. Influence of sea breeze circulation and road traffic emissions on the relationship between particle number, black carbon, PM1, PM2.5 and PM2.5-10 concentrations in a coastal city. Atmospheric Environment 42, 6523–6534.

Schwarz, J.P., Gao, R.S., Fahey, D.W., Thomson, D.S., Watts, L.A., Wilson, J.C., Reeves, J.M., Darbeheshti, M., Baumgardner, D.G., Kok, G.L., Chung, S.H., Schulz, M., Hendricks, J., Lauer, A., Kärcher, B., Slowik, J.G., Rosenlof, K.H., Thompson, T.L., Langford, A.O., Loewenstein, M., Aikin, K.C., 2006. Single-particle measurements of midlatitude black carbon and light-scattering aerosols from the boundary layer to the lower stratosphere. Journal of Geophysical Research: Atmospheres 111, D16207. http://dx.doi.org/10.1029/2006JD007076.

Schwarz, J.P., Gao, R.S., Spackman, J.R., Watts, L.A., Thomson, D.S., Fahey, D.W., Ryerson, T.B., Peischl, J., Holloway, J.S., Trainer, M., Frost, G.J., Baynard, T., Lack, D.A., de Gouw, J.A., Warneke, C., Del Negro, L.A., 2008. Measurement of the mixing state, mass, and optical size of individual black carbon particles in urban

and biomass burning emissions. Geophysical Research Letters 35, L13810. http://dx.doi.org/10.1029/2008GL033968.
Sharma, R.K., Bhattarai, B.K., Sapkota, B.K., Gewali, M.B., Kjeldstad, B., 2012. Black carbon aerosols variation in Kathmandu valley, Nepal. Atmospheric Environment 63, 282–288.
Shiraiwa, M., Kondo, Y., Moteki, N., Takegawa, N., Sahu, L.K., Takami, A., Hatakeyama, S., Yonemura, S., Blake, D.R., 2008. Radiative impact of mixing state of black carbon aerosol in Asian outflow. Journal of Geophysical Research: Atmospheres 113, D24210. http://dx.doi.org/10.1029/2008JD010546.
Stabile, L., Fuoco, F.C., Buonanno, G., 2012. Characteristics of particles and black carbon emitted by combustion of incenses, candles and anti-mosquito products. Building and Environment 56, 184–191.
Suglia, S.F., Gryparis, A., Schwartz, J., Wright, R.J., 2008. Association between traffic-related black carbon exposure and lung function among urban women. Environmental Health Perspectives 116, 1333–1337.
Tsai, C.J., Liu, C.N., Hung, S.M., Chen, S.C., Uang, S.N., Cheng, Y.S., Zhou, Y., 2012. Novel active personal nanoparticle sampler for the exposure assessment of nanoparticles in workplaces. Environmental Science and Technology 46, 4546–4552.
Viidanoja, J., Kerminen, V.M., Hillamo, R., 2002a. Measuring the size distribution of atmospheric organic and black carbon using impactor sampling coupled with thermal carbon analysis: method development and uncertainties. Aerosol Science and Technology 36, 607–616.
Viidanoja, J., Sillanpää, M., Laakia, J., Kerminen, V.M., Hillamo, R., Aarnio, P., Koskentalo, T., 2002b. Organic and black carbon in $PM_{2.5}$ and $PM_{10}$: 1 year of data from an urban site in Helsinki, Finland. Atmospheric Environment 36, 3183–3193.
Virkkula, A., Mäkelä, T., Hillamo, R., Yli-Tuomi, T., Hirsikko, A., Hämeri, K., Koponen, I.K., 2007. A simple procedure for correcting loading effects of aethalometer data. Journal of the Air & Waste Management Association 57, 1214–1222.
Wang, Y., Hopke, P.K., Rattigan, O.V., Zhu, Y., 2011. Characteristic of ambient black carbon and wood burning particles in two urban areas. Journal of Environmental Moritoring 13, 1919–1926.
Watson, J.G., Chow, J.C., Chen, L.W.A., 2005. Summary of organic and elemental carbon/black carbon analysis methods and intercomparisons. Aerosol and Air Quality Research 5, 65–102.
Weingartner, E., Saathoff, H., Schnaiter, M., Streit, N., Bitnar, B., Baltensperger, U., 2003. Absorption of light by soot particles: determination of the absorption coefficient by means of aethalometers. Journal of Aerosol Science 34, 1445–1463.
Zhang, Q., Streets, D.G., Carmichael, G.R., He, K.B., Huo, H., Kannari, A., Klimont, Z., Park, I.S., Reddy, S., Fu, J.S., Chen, D., Duan, L., Lei, Y., Wang, L.T., Yao, Z.L., 2009. Asian emissions in 2006 for the NASA INTEX-B mission. Atmospheric Chemistry and Physics 9, 5131–5153.